Temperature Dependence of Histidine Ionization Constants in Myoglobin

Shibani Bhattacharya and Juliette T. J. Lecomte
Department of Chemistry and the Center for Biomolecular Structure and Function, The Pennsylvania State University, University Park, Pennsylvania 16802 USA

ABSTRACT   The standard enthalpy of ionization of six titratable histidines in horse metaquomyoglobin was determined by repeating proton NMR titrations as a function of temperature and using the van't Hoff relationship. It was found that $\Delta H°$ varies between 16 and 37 kJ mol^{-1} in the protein, compared with a value of 29 kJ mol^{-1} in free histidine. The standard entropy change was evaluated by combining the enthalpy and free energy changes derived from the pK_a values. Although the entropy change could not be precisely and accurately obtained by this method, it could be established that it spans a wide range, from -60 to 0 J K^{-1} mol^{-1}, about the value of -23 J K^{-1} mol^{-1} for the free histidine. The entropy change was used within the framework of enthalpy-entropy compensation to partition the solvation component from the standard thermodynamic quantities for each of the titrating residues. It was shown that the partitioning of the values in the protein is not readily understood in terms of solvent accessibility or electrostatic interactions. The contribution of solvation effects to the temperature response appeared to be significant only in the case of His-119 and His-48. The standard quantities were also used to explore the energetics of proton binding in the native state at temperatures below the onset of thermal denaturation.

INTRODUCTION

The main contributors to electrostatic energy in proteins are charged groups in their interactions with each other and with the surrounding medium. The total charge of a protein, and its electrical free energy, are affected principally by three variables: the pH, the salt concentration, and the temperature of the solution. Because electrostatic interactions differ in the folded and unfolded states of the protein, changing any of these variables influences the stability of the native fold (Tanford, 1957; Tanford and Kirkwood, 1957; Dill, 1990; Stigter and Dill, 1990; Allewell and Oberoi, 1991). Temperature, the variable of interest in this study, has been systematically investigated in concert with pH to map the free energy profile of several water-soluble globular proteins and derive general principles of protein stability (Dill, 1990; Privalov, 1979). It has been established through calorimetric measurements that hydration of polar and nonpolar residues is a reckoning factor in the transition from folded to unfolded state (Makhatadze and Privalov,

1993; Privalov and Makhatadze, 1993; Makhatadze and Privalov, 1994). In view of the participation of specific residues in charge-charge and charge-solvent interactions, a microscopic characterization of representative proteins is desirable to complement the macroscopic calorimetric information.

A powerful approach to a detailed electrostatic description consists in comparing the properties of proteins differing by single mutations at chargeable sites. Staphylococcal nuclease has been subjected to this method exhaustively to evaluate the mean contribution of electrostatic free energy by residue type (Meeker et al., 1996). The drawback of the mutagenesis analysis is that side chain replacements invariably perturb more factors than charge and hydration. Thus, for the study of specific sites, it may lead to ambiguous results. An alternate approach is the direct observation of ionizable residues within the protein by a spectroscopic method capable of resolving sites and monitoring structural changes and charged states. Nuclear magnetic resonance (NMR) spectroscopy is often adequate for this purpose.

Most NMR studies of ionizable groups concentrate on free energy determination via pK_a measurements at a single temperature (Khare et al., 1997), and there are few instances where the enthalpic and entropic contributions have been resolved (Cohen, 1969; Roberts et al., 1969; Westmoreland et al., 1975; Schaller and Robertson, 1995). The solvation properties of an ionizable group in the protonated state differ from those of the ionizable group in the unprotonated state plus free proton. As a consequence, the energetics of hydration are contained in the thermodynamic description of protonation-deprotonation equilibria. The entropic change associated with proton binding are expected to reflect mostly differential solvation effects. Partitioning the free energy into individual contributions therefore offers a means to discriminate solvation from other effects. This distinction is necessary for the complete thermodynamic

Abbreviations used: apoMb, apomyoglobin; 1D, one-dimensional; 2D, two-dimensional; DIPSI, decoupling in the presence of scalar interactions; DQF-COSY, double quantum-filtered correlation spectroscopy; DSS, sodium 2,2-dimethyl-2-silapentane-5-sulfonate; GARP, globally optimized alternating phase rectangular pulse; HMQC, heteronuclear multiple quantum coherence; Mb, myoglobin; MbCO, carbonmonoxymyoglobin; metMb, ferrimyoglobin; metaquoMb, metMbH$_2$O, metMb^{2}H$_2$O, metaquomyoglobin; NMR, nuclear magnetic resonance; NOE, nuclear Overhauser effect; NOESY, two-dimensional nuclear Overhauser spectroscopy; TOCSY, total correlation spectroscopy; TPPI, time proportional phase incrementation.

representation of solvation and desolvation of protein surfaces and all equilibria linked to ionization equilibria.

The transition between unfolded and folded state has attracted the most attention. Under normal conditions, electrostatic forces do not drive the folding reaction (Dill, 1990) and contribute little to the net stability of the native fold (Dill, 1990; Meeker et al., 1996), but they play a role in conditioning the behavior of the protein when exposed to changes in external variables. The pre-denaturational changes induced by temperature, though not dramatic (Privalov, 1979), are caused in part by the ionization reaction of titratable residues and poise the protein for unfolding. This native state pre-transition region remains poorly characterized by theory and experiment. The thermodynamic parameters for the dissociation of ionizable functional groups found in proteins are known (Edsall, 1958). Among the ionizable side chains, histidine residues are of special importance because their dissociation constant is close in value to neutral pH. It is the objective of this work to inspect the thermodynamic properties of histidines within a folded protein and to investigate their role in the pre-denaturational range of temperature.

The standard thermodynamic parameters for histidine ionization can be obtained by varying the temperature and following the response of the equilibrium constant. $\Delta H°$ at temperature T is given by the van't Hoff relation:

$$\left(\frac{\partial \ln K_{a,T}}{\partial(1/T)}\right)_P = -\frac{\Delta H°}{R} \tag{1}$$

and similarly, $\Delta S°$ can be determined by using:

$$\left(\frac{\partial T \ln K_{a,T}}{\partial T}\right)_P = \frac{\Delta S°}{R}. \tag{2}$$

When $\Delta H°$ and $\Delta S°$ are independent of T, i.e. $\Delta Cp° = 0$, measurements of the pK_a at different temperatures yield the answers through simple linear relations between pK_a and $1/T$ or $T \times pK_a$ and T. For any ionization reaction with charge conservation, such as the titration of basic groups, $\Delta Cp°$ is expected to be small (Edsall, 1958), and the assumption is justified at least in the first order. The ionization of acidic groups differs in that it alters the total number of charges and is associated with a nonnegligible $\Delta Cp°$. The enthalpic term is sensitive to all external factors that influence the bond energies, including dielectric constant and solvation. In contrast, the entropy change for a simple proton transfer reaction is dominated by the solute-solvent interactions (Edsall, 1958).

One of the important manifestations of the solute-solvent interactions in a homologous solute series is enthalpy-entropy compensation (Lumry and Rajender, 1970). A wide range of published examples suggests this phenomenon to be the rule for reactions in solvents capable of forming hydrogen bonds. The thermodynamic significance of the effect lies in the partial compensation of the total enthalpy

by entropy whereby the solvent contribution is masked in the free energy of dissociation. Thus, measurements of $\Delta G°$ and $\Delta H°$ for the ionization of histidines might offer an approach for evaluating solvent enthalpic contributions. With data collected on individual side chains in a protein, it should be possible to explore the consequences of solvation and the limitations of quantifying compensatory effects.

The present study tests the usefulness of proton NMR spectroscopy for extracting thermodynamic parameters. Specifically, it seeks to determine the range of enthalpies of ionization of histidines in a protein historically used for thermodynamic and electrostatic investigations, i.e., myoglobin (Mb). Metaquomyoglobin (metaquoMb) is a nonfunctional form of myoglobin where the sixth coordination site of the octahedral ferric complex is occupied by a water molecule. Of the 11 histidines of horse metaquoMb (the species used in this study), 6 titrate in the accessible pH range and their $C\epsilon1\underline{H}$ and $C\delta2\underline{H}$ signals can be followed by NMR spectroscopy (Cocco et al., 1992). Each of these histidines is in a unique environment with respect to nearby charges and solvent accessibility (Evans and Brayer, 1990). It is shown that proton NMR data can be used for resolving the free energy of ionization into enthalpic and entropic components in Mb. The partitioning of $\Delta H°$ and $\Delta S°$ into components with contributions from the protein and the solvent offers insight into how the structure modulates thermodynamic properties.

MATERIALS AND METHODS

Protein samples and pH titrations

Myoglobin from horse (*Equus caballus*) skeletal muscle and all other chemicals was purchased from Sigma Chemical Co. (St. Louis, MO), except for deuterated compounds, which were from Isotec (Miamisburg, OH). Horse Mb was desalted by repeated cycles of dialysis against distilled water and lyophilization. Most exchangeable protons were replaced with deuterium by incubating the purified protein in ^2H_2O at neutral pH for 12 h at room temperature and then lyophilizing it. This step was repeated twice. The absence of bound metal ions was confirmed by comparing spectra of the protein before and after passage over Chelex-100.

For titration purposes, the concentration of the protein samples was ~3 mM in 99.9% ^2H_2O containing 0.2 M NaCl. The total sample volume (~1.8 ml) was divided in two parts for titration in the acid and alkaline range, respectively. The pH of the sample was changed in small increments of 0.15–0.20 units using 0.5 M ^2HCl (0.2 M NaCl) and 0.5 M NaO^2H (0.2 M NaCl). All pH measurements were performed using a 3-mm Ingold combination electrode (6030–1M) and a Beckmann $\phi70$ pH meter. The samples and buffers were maintained at constant temperature (±0.1 K) in a Lauda RCS-6 constant temperature bath. The pH was measured before and after each NMR spectrum was collected. The two readings did not differ by more than 0.02 unit through most of the pH range. At the extremes of the pH scale (<5.2 and >8.5), the difference was of the order of 0.05 unit. In all cases, the second reading was considered to be more accurate and used for data analysis. Each titration was repeated twice at five different temperatures to test the reproducibility of the data. Within the bounds of experimental uncertainty and the small differences in T between two data sets nominally at the same temperature, the agreement between the fitted pK_a values was within 0.05 unit.

NMR spectroscopy

The 1D and 2D NMR spectra were acquired on a Bruker AMX2–500 spectrometer operating at a ^{1}H frequency of 500.13 MHz and a ^{13}C frequency of 125.76 MHz. T was calibrated before and after each titration by using neat ethylene glycol (Martin et al., 1980). The difference between the two values never exceeded 0.5 K. The temperature of the water bath was set to match the temperature of the NMR probe at the beginning of the titration. The spectrum at each pH point was collected with a 1.2-s presaturation of the residual ^{1}H^{2}HO signal. A total of 256 transients were collected with a spectral width of 7042 Hz and 8192 real points. Homonuclear NOESY data and TOCSY data with relaxation compensated DIPSI mixing schemes (Cavanagh and Rance, 1992), 2Q data (Rance and Wright, 1986), and DQF-COSY data (Derome and Williamson, 1990) were collected on 4 mM (0.2 M NaCl) protein samples in 90% ^{1}H$_2$O/10% ^{2}H$_2$O (v/v) at 298 K and 322 K. TOCSY and NOESY data used a modified WATERGATE (Piotto et al., 1992) for water suppression, and the other experiments used a 1.2-s presaturation of the residual ^{1}H^{2}HO line. Acquisition parameters for these experiments were as reported elsewhere (Cocco et al., 1992; Kao, 1994; Lecomte et al., 1996).

Natural abundance HMQC spectra (Müller, 1979) were acquired on a 12 mM Mb (0.2 M NaCl) sample at 313 K. The spectral width in the ^{13}C dimension was 12,500 Hz centered at 125.770489 MHz (101 ppm). A total of 160 t_1 increments were collected in the TPPI-States mode, with 192 transients per point. The 1/2J delay was set to 3.3 ms. The residual ^{1}H^{2}HO signal was presaturated as above, and GARP decoupling was applied during acquisition.

All data processing was carried out with FELIX (Molecular Simulations, San Diego, CA). Homonuclear data were treated as previously reported (Cocco et al., 1992; Kao, 1994; Lecomte et al., 1996). For the heteronuclear data sets, 30 additional points were predicted linearly in the indirect dimension. Shifted squared-sinebell windows were applied in both dimensions (typically the shifts were 60° in t_2 and 90° in t_1); data were zero-filled so as to generate a final transform with 3.4 Hz/point resolution in the proton dimension and 12.2 Hz/point in the carbon dimension. Proton chemical shifts were referenced indirectly to DSS through the ^{1}H^{2}HO line using the values recommended in Wishart et al., 1995. Carbon chemical shifts were referenced to DSS by the method of Live et al. (1984). In the text, the nuclei of interest are underlined wherever ambiguity could arise.

Titration data analysis

The pK$_a$ values for each detectable histidine were obtained as a function of T from 1D proton data. In the simplest cases, the chemical shift of the carbon-bound histidine ring protons can be fit as a function of pH to a modified Henderson-Hasselbalch equation (Markley, 1975):

$$\delta_{obs} = \delta_{His} + (\delta_{His^+} - \delta_{His}) \frac{10^{n(pK_a - pH)}}{1 + 10^{n(pK_a - pH)}}. \tag{3}$$

In this equation, δ_{His}, δ_{His^+}, n (Hill coefficient), and pK$_a$ (apparent ionization constant, pH at which 50% of the given histidine population is protonated) are adjustable parameters. Equation 3 is valid on the conditions that 1) the protonation-deprotonation process is fast on the NMR time scale and leads to a chemical shift δ_{obs} that is a weighted average of δ_{His} (neutral imidazole chemical shift) and δ_{His^+} (imidazole cation chemical shift), and 2) the chemical shift δ_{obs} is not directly influenced by the titration of residues other than the one under observation.

The two conditions described above are not strictly observed by all histidines in metaquoMb. The protein undergoes hemic acid dissociation (loss of a hydrogen ion by the liganded water) near pH 8.8 (George and Hanania, 1952; Brunori et al., 1968). The high-to-low-spin alkaline transition is observed in the proton chemical shifts of many residues, including a few histidines (Carver and Bradbury, 1984; Cocco et al., 1992). When this transition is detected in a chemical-shift-versus-pH profile, a second Henderson-Hasselbalch term is necessary. The pK$_a$ of this transition can be extracted when the two titration steps are well separated (as for His-48).

The hemic acid pK$_a$ can then be fixed to this value for residues with overlapping histidine and alkaline transitions. This procedure is preferred over truncating the data sets to obtain accurate δ_{His} values when high and low pH transitions are not completely resolved. Hemic acid dissociation has a $\Delta H°$ of ~25 kJ mol^{-1} (George and Hanania, 1952), comparable to $\Delta H°$ of histidine ionization (29 kJ mol^{-1}; Boschcov et al., 1983). As a result, both transitions move in parallel when T is changed.

His-48 and His-113 have a relatively low pK$_a$ (Cocco et al., 1992). At temperatures above 298 K, there are insufficient data points to define accurately the acid baseline, δ_{His^+}. To circumvent this problem, the data were fitted by fixing the total chemical shift excursion ($\Delta\delta = \delta_{His^+} - \delta_{His}$) to its 288 K value. The assumption that $\Delta\delta$ is independent of T is verified for residues exhibiting a well-defined acid baseline under all conditions. This treatment is successful also because the titratable residues happen to be sufficiently remote from the paramagnetic center that differential dipolar effects on neutral and protonated forms, if any, are small.

His-116 Cϵ1H at all temperatures has a chemical-shift-versus-pH profile poorly accounted for by Eq. 3 as judged through a systematic and reproducible pattern of residuals. One explanation for the inadequacy of Eq. 3 is that the condition of fast exchange is not obeyed. Although a single His-116 Cϵ1H signal can be followed through the transition, severe broadening is observed around the pK$_a$ value. This exchange broadening is a potential cause for distortions of the titration curve (Sudmeier et al., 1980), and its consequences were explored.

Three mechanisms contribute to the protonation-deprotonation equilibrium of imidazole rings: 1) loading of a proton on the neutral group, 2) loading of a hydroxide ion on the charged group, 3) collisions with buffer or other protein molecules (Sudmeier et al., 1980). With each of these processes are associated rate constants, which may be retarded compared with those in a model peptide because of diminished site accessibility in the protein. A FORTRAN program was written to simulate the titration curves according to the equations contained in Sudmeier et al. (1980). Line widths and line positions were calculated as functions of pH given realistic limiting line widths, chemical shift separation, pK$_a$, and rate constants for proton loading and hydroxide loading. The contribution from exchange was neglected as the solutions contained a low concentration of the protein and no buffer. To approximate the curve of His-116 Cϵ1H, the rates for H$^+$ and OH$^-$ loading had to be decreased below the accepted value of 2 × 10^{-12} M^{-1} s^{-1}. The simulations demonstrate that with a moderate retardation of the on-rate constants, the chemical shift curve deviates noticeably (though not extremely) from the trace produced with Eq. 3 and that such deviation can account for at least some of the residuals. When the His-116 Cϵ1H simulated titration curves are fitted to Eq. 3, the fitted pK$_a$ differs from the input pK$_a$ only by a small amount (<0.04).

Another explanation for the deviation is the direct influence of a neighboring titrating group on the chemical shift observable. This behavior has been reported for many compounds, and appropriate equations have been developed (Shrager et al., 1972). The data for His-116 are satisfactorily fitted with the sum of two Henderson-Hasselbalch equations with pK$_a$ values approximately 1.3 U apart. The equation contains five parameters: acid and basic chemical limits, two pK$_a$ values, and a weighing factor that quantifies the contribution of each pK$_a$ to the observed chemical shift response. To ensure that the use of a different model with one additional parameter made a significant change to the quality of the fit, the results obtained in both fashions were evaluated in an approximate F test. For His-116, the simpler model can be rejected at better than the 95% confidence level.

The ambiguous case of His-116 was explained to illustrate the complexity and limitations of ^{1}H titration curves. At a spectrometer frequency of 500 MHz, exchange may distort the titration profiles from Eq. 3. Accurate line width measurements cannot readily be performed, and the model used to simulate the spectra may be oversimplified. Therefore, the contribution from the exchange effects is difficult to evaluate. Furthermore, equally elusive direct or indirect effects from simultaneous titrations could also distort the curve. These problems justify the following operational rules: 1) the modified Henderson-Hasselbalch equation is used as long as a single signal is obtained at all pH values (the case for all Mb histidines); 2) the pK$_a$ values should be considered as best apparent estimates, partic-

ularly where broadening occurs; 3) the Hill coefficient, adjusted in the fitting so as to minimize the deviations caused by shape distortion, is an ad hoc parameter that cannot be compared meaningfully from residue to residue or titration to titration.

Enthalpy and entropy calculations

The pK_a values were measured at five temperatures: 288.1 K, 299.5 K, 305.8 K, 312.4 K, and 322.0 K. $\Delta H°$ was estimated from a linear least-squares fit of pK_a versus $1/T$ using Eq. 1 with appropriate conversion factors and the assumption that $\Delta Cp°$ is zero for the ionization process. The precision of the data does not justify the addition of a heat capacity parameter in the fit. $\Delta S°$ was estimated from a linear least-squares fit of $T \times pK_a$ versus T using Eq. 2 with appropriate conversion factors. Both $C\delta 2\underline{H}$ and $C\epsilon 1\underline{H}$ signals could in principle be used for the calculations of $\Delta H°$ and $\Delta S°$. Whenever possible, the $C\epsilon 1\underline{H}$ signal was selected because of its larger $\Delta\delta$ and better residual patterns. His-119 was an exception to this, as its $C\epsilon 1\underline{H}$ is not detectable through the transition; His-119 $C\delta 2\underline{H}$ was followed instead.

Error calculations

Myoglobin pK_a values were reported previously to ± 0.1 pH unit (Cocco et al., 1992; Kao, 1994) to account for all experimental variables and to set expectations if the titrations were repeated by others. In the present study, the pK_a values are used for quantitative purposes; therefore, it was necessary to inspect the uncertainty range. Titrations on horse Mb and the closely related sperm whale protein were repeated three times at room temperature (this work; Kao, 1994); the data sets yield pK_a values contained within a 0.05 pH unit window. In most cases, the average standard deviation obtained from the fits to Eq. 3 is lower than half this value.

The method of Kelly and Holladay (1990) was applied as a control. In brief, 25 titrations were simulated for His-113 (data set truncated on the acid side) with normal distribution of errors compatible with experimental observations (± 0.01 pH unit and ± 0.003 ppm). Each of the generated curves was then fitted to Eq. 3, and the average pK_a value and its range determined. The standard deviation was found to be ± 0.03 pH unit. Thus, the random error is small even for the low pK_a residues, and systematic errors dominate. For this study, pK_a values are estimated at ± 0.05 pH unit, except for the low pK_a histidines where the lack of an acid baseline increases the range to ± 0.07 pH unit. Because of the nonlinear least-squares routine, the upper and lower bounds of the 95% confidence interval are not symmetrically distributed around the value. The χ^2 method detailed in Shoemaker et al. (1989) for asymmetrical intervals was applied to ascertain that even for low pK_a histidines, the interval is contained within the assumed experimental error. $\Delta G°$ extremes were calculated from the upper and lower pK_a values.

The least-squares procedure yielding $\Delta H°$ (or $\Delta S°$) returns standard deviations that measure the goodness of the fit to an equation with $\Delta Cp° = 0$. In the van't Hoff graph (see Fig. 3), this standard deviation is depicted with the understanding that linearity is implicit in the chosen mode of representation. Table 3 includes estimates of lower and upper values, as obtained graphically through the uncertainty on pK_a (or $T \times pK_a$).

RESULTS

Spectral assignments

Of the eleven histidines in horse metaquoMb, only three, His-64 (E7, distal), His-93 (F8, proximal), and His-97 (FG3), are not readily detectable at any pH owing to their proximity to the paramagnetic heme center. The remaining eight are observable by proton NMR spectroscopy and their $C\delta 2\underline{H}$ and $C\epsilon 1\underline{H}$ signals could be assigned at low pH with 2D methods (Cocco et al., 1992). These histidines are His-24 (B5), His-36 (C1), His-48 (CD6), His-81 (EF4), His-82 (EF5), His-113 (G14), His-116 (G17), and His-119 (GH1). At intermediate and high pH values, the $C\epsilon 1\underline{H}$ of His-82 and His-119, and the $C\delta 2\underline{H}$ of His-36 are difficult to follow.

To confirm and complete the proton assignments of the detectable imidazole groups, natural abundance ^{13}C data were collected as a function of pH at 313 K. Two representative ^1H-^{13}C HMQC spectra are shown in Fig. 1, A (pH 5.6) and B (pH 8.4), to illustrate the spectral resolution obtained with this approach. The correlation peaks and known proton chemical shifts allowed for assignment of $C\epsilon 1$ and $C\delta 2$ signals and for coarse ^{13}C titration curves to be derived from the data. These curves are shown in Fig. 2, A ($C\epsilon 1$) and B ($C\delta 2$); they were useful to assign proton signals in the pH ranges where overlap interfered with the analysis of 1D data. Furthermore, the line broadening through the titration is not as detrimental for the carbon signals as for the proton ones, and it was possible to follow the $C\delta 2H$ correlation peak from His-36 (yielding one of the best-defined ^{13}C curves) and the $C\epsilon 1H$ correlation peak from His-82 (confirming little variability of chemical shift). The low-resolution 2D ^1H-^{13}C spectra were not utilized to determine precise ionization constants; the data were qualitatively consistent with the conclusions based on proton spectra except in one case (see below). In addition to securing assignments, the ^{13}C data also provided insights on the tautomeric state of the imidazole rings.

Structural considerations

Effect of temperature and pH variations

A primary concern when considering the temperature dependence of an ionization process is the stability of the protein and the constancy of its structure over the range of explored conditions. Thermal and pH denaturation data are available for horse metMbH$_2$O (Cho et al., 1982) and the structurally homologous sperm whale metMbH$_2$O (Acampora and Hermans, 1967; Privalov et al., 1986). These studies provide boundaries to confine pH and T so that the native state is the predominant form under analysis. No evidence of denaturation was found in any of the collected spectra. Thus, the characterization applies to the pre-denaturation zone of Mb.

Changes in T and pH are possible causes for local perturbations of the structure and dynamics of the native state. A comparison of the 80 K metMbH$_2$O structure (Hartmann et al., 1982) and the 260 K MbCO structure (Kuriyan et al., 1986), with molecular simulations of MbCO at 325 K and 80 K, have revealed the largest T-dependent structural changes of the protein to be restricted to loops CD, EF, and helix E (Kuczera et al., 1990). The structural effects of pH on metMbH$_2$O have been probed by x-ray crystallography as well (Yang and Phillips, 1996). The same regions of the protein are affected when the pH is lowered below 5.
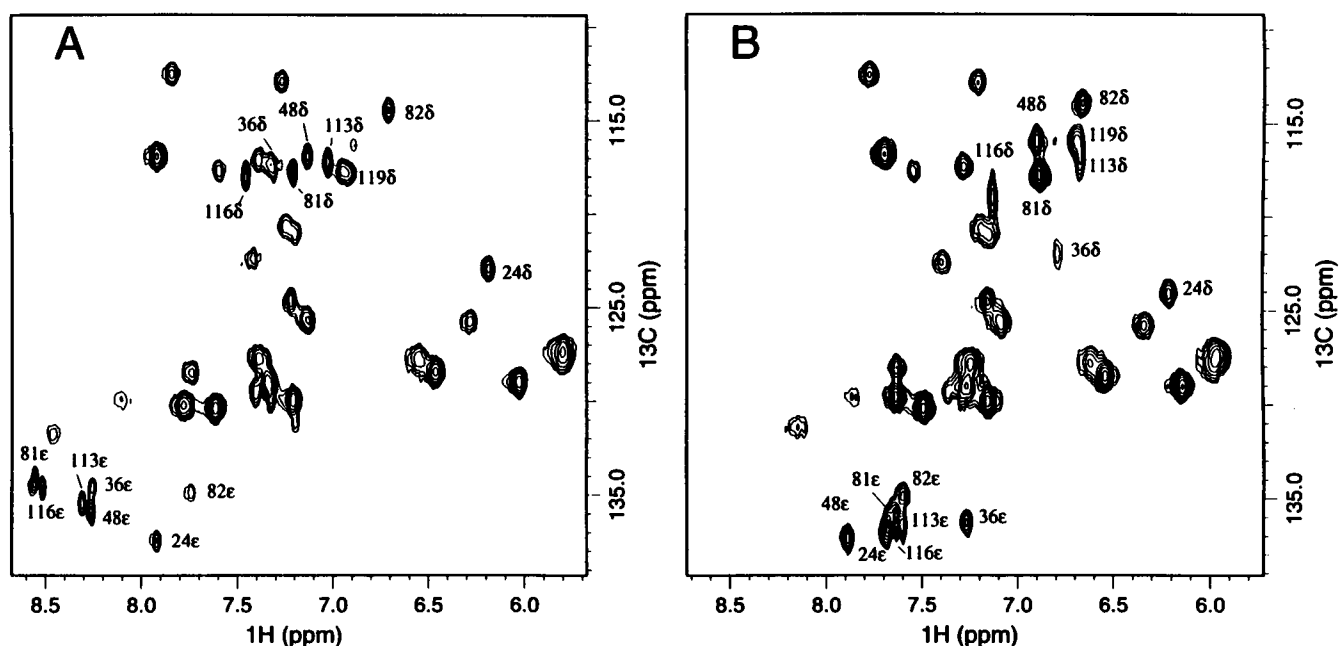
FIGURE 1 ^{1}H–^{13}C HMQC spectrum of horse metaquoMb in 99% ^{2}H$_2$O, at 313 K, showing the aromatic region. Cross-peaks due to histidines Cδ2H and Cε1H are labeled. (A) pH 5.58; (B) pH 8.43.

To investigate the response of the structure in solution, NOE data were collected up to 322 K and at high and low pH. Several NMR spectral indicators (chemical shift, line width, intensity, and dipolar contacts) were inspected to ascertain the integrity of the global native fold and test the invariance of the local environments of interest. Particular attention was devoted to the three titrating histidines located in the flexible loops (His-48, His-81, and His-82). Major conformational changes due to elevated T and pH variations were readily ruled out. Subtle changes, which might not be unambiguously reflected in the NOEs, remain possible.

Tautomeric state of observable histidines

The neutral imidazole ring can exist in two possible forms depending on which nitrogen (Nδ1 or Nε2) has an attached proton. The tautomeric state constitutes a necessary piece of information for the interpretation of thermodynamic data (Shire et al., 1974; Botelho et al., 1978; Boschcov et al., 1983; Bashford et al., 1993) and structural details in solution. The tautomeric state of the histidines in sperm whale Mb has been determined using the ^{15}N chemical shift of the imidazole ring nitrogens (Bhattacharya et al., 1997). For the present work on horse Mb, ^{1}H-^{13}C HMQC data served to track histidine signals and to report on the tautomeric state. As pointed out in previous studies of myoglobin (Wilbur and Allerhand, 1977), the sign and magnitude of the chemical shift change experienced by imidazole carbons in model compounds (Reynolds et al., 1973) provide a yardstick to interpret the protein values: a downfield shift of Cε1 and Cγ and an upfield shift of Cδ2 as the pH is raised indicate that the deprotonation favors the Nε2H tautomer. A downfield

shift of Cε1 and Cδ2 along with an upfield shift of Cγ as the pH is raised indicate that the Nδ1H tautomer is favored in the neutral state.

The ^{13}C data obtained with the HMQC sequence yield Cε1 and Cδ2 shifts and are complementary to those published for the Cγ shift (Wilbur and Allerhand, 1977). The difference of the carbon chemical shifts at pH 5.6 and 8.4 (Fig. 1, A and B), the results from model compound studies (Reynolds et al., 1973), and the tautomeric state information for Mb have been compiled in Table 1. Unlike the ^{15}N chemical shift method, for which a single spectrum at a pH where the imidazole ring is uncharged suffices, the ^{13}C chemical shift method relies on differences between imidazole and imidazolium chemical shifts. As the imidazolium form may not be entirely populated at the lowest pH where the protein is native, the ^{13}C method can provide only a qualitative assessment. As will be described below, there are additional drawbacks that make the ^{13}C method occasionally ambiguous. The ^{15}N data on sperm whale Mb and ^{13}C data on horse Mb are in agreement within the limitations of both methods.

Determination of pK$_a$

To determine thermodynamic parameters for individual sites, the pH titrations were performed at five temperatures in the range 288–323 K in the presence of 0.2 M NaCl. At the high end of the T range, the protein tends to remain soluble over a narrow pH window; on the other hand, the lines are sharper and the titration of residues such as His-36 can be monitored more closely. At the low end of the T range, lines are broader and spectral overlap increases, but
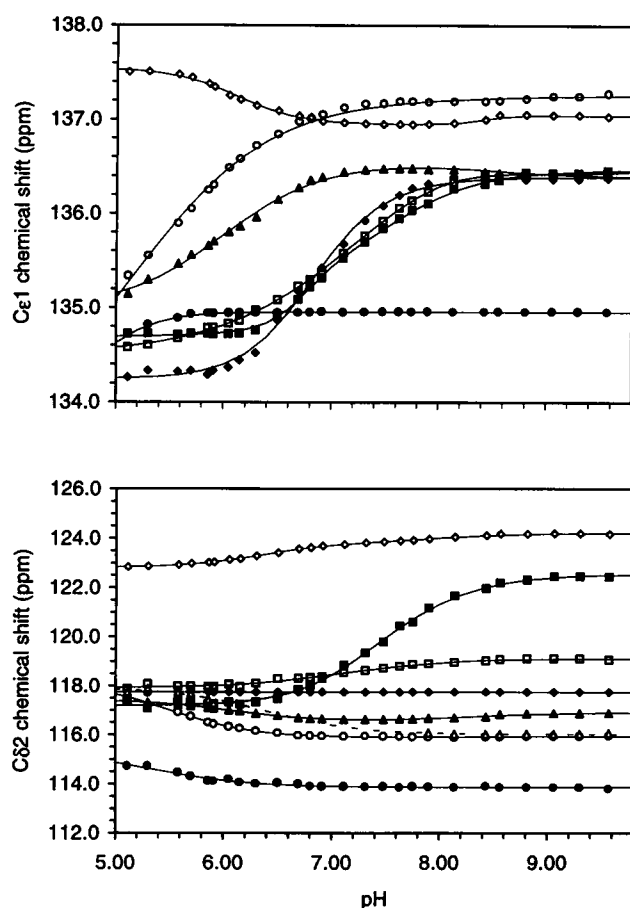
FIGURE 2   Carbon titration curves for the histidines of horse meta-quoMb at 313 K constructed from the data in ^{1}H–^{13}C HMQC spectra as shown in Fig. 1. The assignments were obtained by matching with the known proton assignments (Cocco et al., 1992) and are as follows: His-24, ◇; His-36, ■; His-48, ○; His-81, ◆; His-82, ●; His-113, ▲; His-116, □; His-119, △. The data points are connected by lines to guide the eye. Bottom panel, Cδ2H signals; top panel, Cε1H signals.

modynamic quantities for model compounds and the histidines of metaquoMb.

His-24

His-24 is a masked residue (Breslow, 1964) buried in the protein and interacting strongly with His-119. The 24–119 pair is identified by numerous NOEs to surrounding residues (e.g., Val-17, Asp-20, Val-114, and Leu-115) and to each other (Cocco et al., 1992). Overall, the structures of sperm whale and horse Mb are quite similar. However, one region of marked alterations related to the substitutions His-12(SW)→Asn(Eq) and Arg-118(SW)→Lys(Eq) contains His-24 and His-119 (Evans and Brayer, 1990). Arg-118 in sperm whale Mb stacks over His-24; replacing Arg-118 might result in the weakening of the interactions between the two residues and also between His-24 and the B helix backbone.

His-24 senses two titration events in the native range: near neutral pH and near pH 9. Proton data show that the alkaline transition moves to lower pH as T is raised, in agreement with the positive enthalpy of hemic acid dissociation; the first transition is attributed to His-119 (Dalvit and Wright, 1987; Cocco et al., 1992). The carbon responses at 313 K are shown in Fig. 2. The downfield Cε1 shift upon acidification is unusual for not being observed in any of the model compounds. The ^{13}C chemical shift has two components, one diamagnetic that is proportional to electron density and one paramagnetic that is a function of electron density and degree of mixing of the excited states (Pople et al., 1959; Kalinowski et al., 1991). A meaningful interpretation would require in depth theoretical modeling, which will not be attempted. However, the downfield shift is reminiscent of an effect simply proportional to electron density. This type of contribution can occur away from the site of ionization (Quirt et al., 1974) and might reflect the influence of His-119. An indirect response has also been observed in α-lytic protease (Hunkapiller et al., 1973). The anomalous curve of His-24 is consistent with closely interacting histidines in the horse protein but cautions about the indiscriminate use of ^{13}C shifts when the residue is in a markedly different environment from an aqueous medium.

the protein is capable of withstanding exposure to lower pH. In addition, because the enthalpy of ionization is positive, lowering T raises the pK_a and extends the baseline on the acid side. Thus, the low temperature data allow for a better definition of the curves for residues with a low pK_a.

In what follows, the results are summarized for each histidine, starting with the nontitrating residues and then progressing from the simplest titrating residue to the most complex. The features of each microenvironment have been described elsewhere (Cocco et al., 1992; Bhattacharya et al., 1997). Only the salient properties of the horse variant and the spectral criteria for structural integrity are presented along with the temperature response of the ionization constants where available. To illustrate the consequences of the temperature dependence on the charge carried by the ring, the curves of fraction protonated, Z, versus pH are presented in Fig. 3 for each titratable histidine at each T, and the pK_a values are given in Table 2. Fig. 4 contains the van't Hoff plots constructed from the data, and Table 3 lists the ther-

His-82

His-82 is buried at the interface of the H helix and the EF corner. Characteristic NOEs between the ring of His-82 and Leu-86 ascertain the relative position of 82 throughout the pH range. The ^{15}N data collected on sperm whale Mb (Bhattacharya et al., 1997) confirm that the residue is neutral and in the Nε2H form. A similar situation is expected in the horse protein as the substitution Lys-140(SW)→ Asn(Eq) has no apparent consequence in the solid state structure and the environment of the residue is otherwise conserved (Evans and Brayer, 1990).

TABLE 1   Structural information for model compounds and the observable histidines of metaquoMb

Compound/ residue	$\Delta\delta C\delta 2$*	$\Delta\delta C\varepsilon 1$*	$\Delta\delta C\gamma$*	Tautomeric state[#]	Solvent accessibility[§] (%)	
					Nδ1	Nε2
His	+0.7	−2.4	−4.8	Nε2H (80%)		
Nδ1Me-His	−7.1	−3.4	+2.3	Nδ1H model		
Nε2Me-His	+2.1	−3.5	−6.8	Nε2H model		
His-24	−1.1	+0.5		Nδ1H	0	0
His-36	−5.2	−1.7		Nδ1H (80%)	25	50
His-48	<+1.6	>−1.8		Nε2H	25	45
His-81	≈0	−2.1		Nε2H (80%)	40	100
His-82	>+1.0	<−1.2		Nε2H	10	5
His-113	>+0.6	−1.7		Nε2H (70%)	50	60
His-116	−0.9	−1.7		Nε2H (60%)[¶]	45	5
His-119	>0	NA		Nε2H	25	0

*Value from Reynolds et al. (1973) for the model compounds and from this work for horse metaquoMb at 313 K, 0.2 M NaCl.
[#]As determined by using the $\Delta\delta^{13}$C values and ^{1}H-^{15}N data of Bhattacharya et al. (1997) for the sperm whale protein where the two protein structures are superimposable.
[§]As calculated and normalized to tripeptide values using the x-ray structure 1YMB (Evans and Brayer, 1990) and the procedure of Lee and Richards (1971).
[¶]His-116 differs in solvent accessibility in horse Mb (1YMB) and sperm whale Mb (4MBN). This percentage is estimated on the basis of the negative $\Delta\delta^{13}$Cδ2.

The carbon shifts of His-82 (Fig. 2) display the beginning of a titration event at low pH, and the sign of the deflection is similar to that of His-48 and His-119, in agreement with a Nε2H imidazole tautomer. The proton data show that decreasing T raises the onset of the event to higher pH values, as would be expected for a histidine pK$_a$. Even when T is lowered to 288 K, the inflection point does not move within the observable pH window, and the pK$_a$ estimate remains no more precise than previously reported, between 4 and 5.

His-81 (Fig. 3 A)

His-81 is also in the EF loop but exposed to solvent. As a corollary His-81 has few NOEs to orient the side chain with respect to the protein surface. His-81 is the simplest of the titrating residues, with no sensitivity to hemic acid dissociation and a normal pK$_a$ value (Cocco et al., 1992). In the carbon titration, the chemical shift deviations are similar to those observed for free histidine. The normalized carbon and proton titration curves are nearly coincident. The tautomeric state of His-81 in the sperm whale protein is close to that of a free histidine (Bhattacharya et al., 1997), and the same is expected of the residue in the horse protein as confirmed by ^{13}C shifts. His-81 has an enthalpy of ionization of 31 kJ mol^{-1}, within error of the value for a free histidine residue (Boschcov et al., 1983). In this instance, a site-resolved enthalpy of ionization is reliably extracted from the proton titration curves. The entropy of ionization is −28 J K^{-1} mol^{-1}, also comparable to that of a free histidine.

His-48 (Fig. 3 B)

His-48 shows few dipolar contacts, notably to Leu-49 and Phe-46. In the sperm whale protein, His-48 adopts the Nε2H

tautomer almost exclusively in the neutral form. The carbon data of Fig. 2 indicate a preference to form the Nε2H tautomer of the neutral imidazole. His-48 is sensitive to a high pH event, taken to be hemic acid dissociation (Carver and Bradbury, 1984; Cocco et al., 1992). The temperature dependence of this second transition is in agreement with this assumption. His-48 has the lowest measured pK$_a$ and the lowest enthalpy value, 16 kJ mol^{-1} (Table 3). Even though the uncertainty on the enthalpy measurement is high, the value is significantly different from that of the free histidine model.

His-119 (Fig. 3 C)

In the 24–119 hydrogen bond identified in the solid state, the proton is shared between the Nε2 sites of the two residues, leaving the Nδ1 site of His-119 available for protonation. The neutral form of His-119 dominates above pH 6.4 at room temperature in the absence of salt and should be mostly Nε2H tautomer. This is indeed observed in the sperm whale protein (Bhattacharya et al., 1997). The carbon data are incomplete for this residue because of excessive broadening through the transition, but the change of chemical shift experienced by Cδ2 is consistent with the formation of Nε2H imidazole. The enthalpy of ionization is determined to be a low 20 kJ mol^{-1} and the entropy of ionization to be −58 J K^{-1} mol^{-1}.

His-113 (Fig. 3 D)

His-113 is moderately exposed to the solvent and NOEs to Val-114 and His-116 are observed. The proximity of Arg-31 explains the low pK$_a$ (Gurd et al., 1980). The carbon chemical shift differences support a tautomeric mixture similar to that of His-81. The enthalpy of ionization is 23 kJ mol^{-1}, comparable to that of His-119.
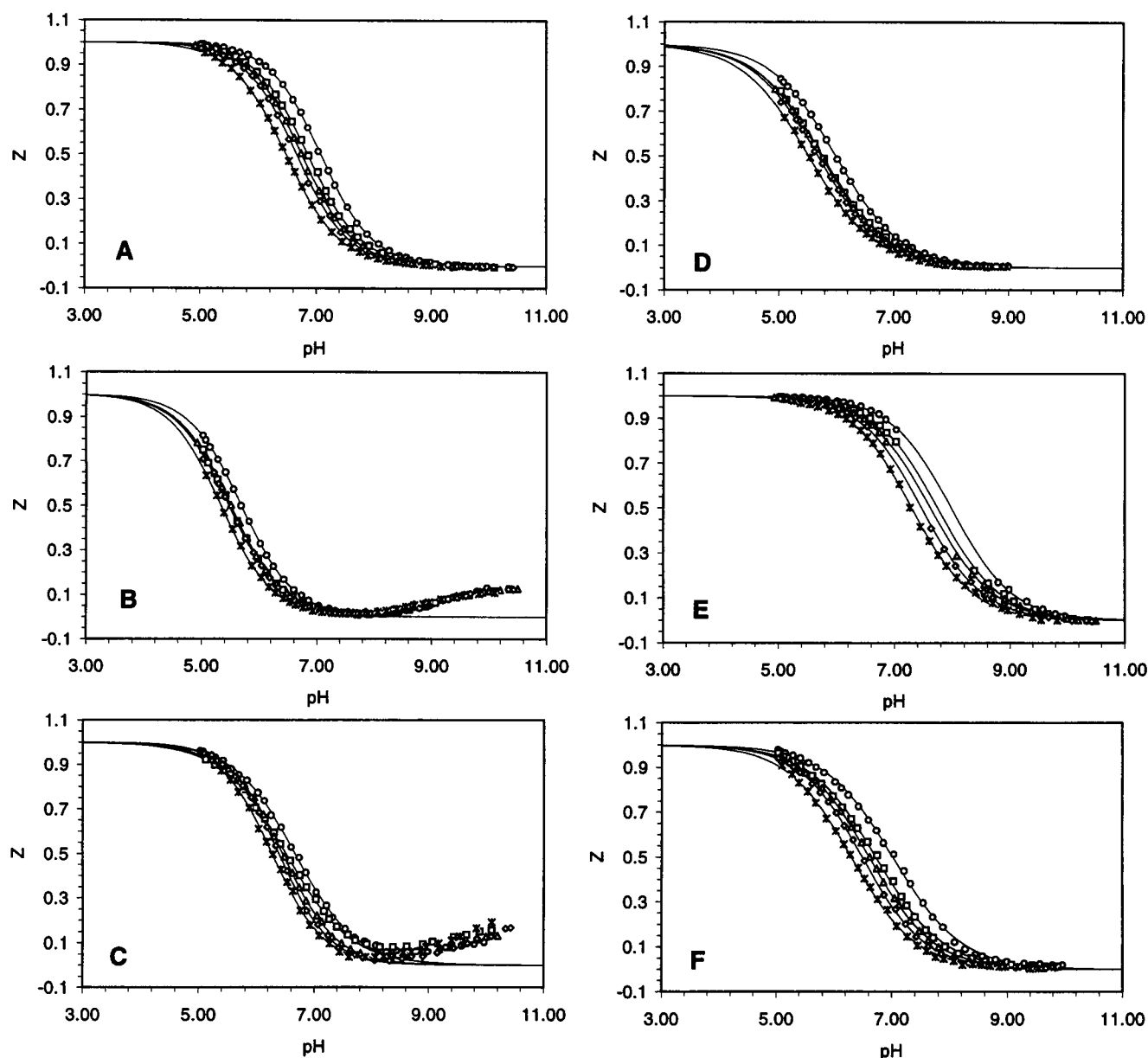
FIGURE 3 Fraction of protonated histidine as a function of pH and temperature. (A) His-81; (B) His-48; (C) His-119; (D) His-113; (E) His-36; (F) His-116. Temperatures were as follows: 288.1 K, O; 299.5, □; 305.8, △; 312.4, ◇; 322.0, *. The lines represent the fit to a simple modified Henderson-Hasselbalch equation with pK_a listed in Table 2. Hill coefficients were independent of temperature and set to 0.93 (His-81), 0.96 (His-48), 0.88 (His-119), 0.75 (His-113), 0.82 (His-36), and 0.75 (His-116).

His-36 (Fig. 3 E)

His-36 stacks onto Phe-106, and the inter-ring NOEs confirm that the two side chains are nearly parallel. These NOEs are maintained throughout the temperature range. The carbon data are useful as the residue was not observed in the high-pH ^1H-^{15}N HMQC experiments on the sperm whale protein. Marked downfield shifts for both $C\epsilon 1$ and $C\delta 2$ take place as the pH is raised (Fig. 2). These effects are consistent with a high population of the $N\delta 1H$ tautomer. If it is assumed that the model compound values can be used to estimate proportions, His-36 is nearly 90% in the $N\delta 1H$

form. Interestingly, His-36 $C\gamma$ was not identified in the early carbon studies (Wilbur and Allerhand, 1977). The 90% tautomeric mixture is such that this signal should not shift appreciably as the ring titrates. The enthalpy of ionization for this residue is comparatively high, 36 kJ mol^{-1}.

His-116 (Fig. 3 F)

His-116 has diagnostic NOEs to Leu-115 and Phe-123. Its pK_a is normal. The crystal structure indicates higher solvent accessibility at the $N\delta 1$ site than at the $N\epsilon 2$ site (Table 1).

TABLE 2 Titration parameters as a function of temperature for selected resonances of metaquoMb

Residue	Signal	T*	pK_a[#]	SD[§]	Comments[¶]
His-36, ±0.05[‖]	CεlH	288.1	7.99	0.01	mHH; broad
		299.5	7.75	0.01	mHH; broad
		305.8	7.63	0.01	mHH; broad
		312.4	7.48	0.01	mHH; broad
		322.0	7.31	<0.01	mHH; broad
His-48, ±0.07	CεlH	288.1	5.69	<0.01	mHH + HH
		299.5	5.50	<0.01	mHH + HH + Δδ fix
		305.8	5.51	<0.01	mHH + HH + Δδ fix
		312.4	5.48	<0.01	mHH + HH + Δδ fix
		322.0	5.34	<0.01	mHH + HH + Δδ fix
His-81, ±0.05	CεlH	288.1	7.08	<0.01	mHH
		299.5	6.86	<0.01	mHH
		305.8	6.75	<0.01	mHH
		312.4	6.66	<0.01	mHH
		322.0	6.48	<0.01	mHH
His-113, ±0.07	CεlH	288.1	5.99	<0.01	mHH + HH
		299.5	5.76	<0.01	mHH + HH + Δδ fix
		305.8	5.74	<0.01	mHH + HH + Δδ fix
		312.4	5.68	<0.01	mHH + HH + Δδ fix
		322.0	5.52	<0.01	mHH + HH + Δδ fix
His-116, ±0.05	CεlH	288.1	7.02	0.01	mHH; broad
		299.5	6.72	0.02	mHH; broad
		305.8	6.61	<0.01	mHH; broad
		312.4	6.49	<0.01	mHH; broad
		322.0	6.30	0.02	mHH; broad
His-119, ±0.05	Cδ2H	288.1	6.66	0.02	mHH + HH; broad
		299.5	6.51	0.02	mHH + HH; broad
		305.8	6.45	0.01	mHH + HH; broad
		312.4	6.38	0.01	mHH + HH; broad
		322.0	6.27	0.02	mHH + HH; broad

*Temperature as calibrated, ±0.3 K over time of the experiment.

[#]pK_a values from nonlinear least-squares fit.

[§]Standard deviation of the fit.

[¶]mHH, Eq. 3 (modified Henderson-Hasselbalch equation), used for histidine transition; HH, Henderson-Hasselbalch equation, Hill coefficient set to 1, used for alkaline transition; Δδ fix, fixed $\delta_{His}{}^+$ value in the mHH fit; broad, indicates considerable broadening through the transition possibly responsible for deviation from mHH profile.

[‖]Estimated uncertainty due to systematic error (see text).

This is in contrast to the geometry in the sperm whale protein, where the Nδ1 site is buried. The sperm whale Mb ^{15}N data support the preferential population of the Nε2H tautomer but with a contribution from the Nδ1H form higher than in the exposed residue. The carbon data of Fig. 2 show a slight downfield shift of Cδ2 as the pH is raised through the transition of the residue. This also suggests an enhanced contribution of the Nδ1H tautomer. The pK_a is similar in horse and sperm whale Mb (Cocco et al., 1992), and it appears that tautomeric composition and pK_a are not drastically affected by the structural differences.

The high quality of the proton data collected at 288 K revealed a fine feature of the titration of His-116. Most histidines follow a modified Henderson-Hasselbalch profile; they are symmetrical with respect to pH = pK_a and satisfactorily modeled with a Hill coefficient between 0.7 and 1. However, the curves for His-116 display asymmetry that cannot be reproduced with the application of this coefficient. The asymmetry can be explained either by broadening through the titration or by the influence of another titration event (nearby residue or conformational change) or

both (see Materials and Methods). The effect is slight and does not allow for definitive identification. The pK_a values generated from a single modified Henderson-Hasselbalch equation applied to proton and carbon data are generally in qualitative agreement, except for His-116, where the pK_a given by the carbon data is higher than that by the proton data (Fig. 2). The different side chain conformations adopted in sperm whale Mb (Takano, 1977, 1984) and in horse Mb (Evans and Brayer, 1990) at the end of the G helix, and the anomalous curves reinforce that His-116 is in an electrostatically and structurally complex location.

There are precedents for the noncoincidence of proton and carbon curves. In calbindin D_{9k}, lysines were shown to yield different information when observed through these two nuclei (Kesvatera et al., 1996). The carboxylic acid groups of ribonuclease HI also give conflicting values (Oda et al., 1994). As mentioned in the case of His-24, carbon and proton chemical shifts are sensitive to distinct influences (Pople et al., 1959; Quirt et al., 1974). In Mb, the total proton chemical shift excursion varies little from titrating site to titrating site, and it is proposed that the main event
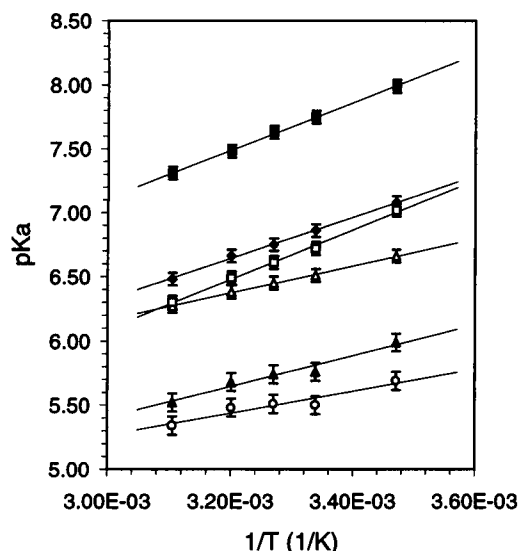
FIGURE 4 van't Hoff plot for the six histidines shown in Fig. 3: His-36, ■; His-48, ○; His-81, ◆; His-113, ▲; His-116, □; His-119, △. Error bars represent the standard deviation listed in Table 3. This plot was used to estimate the upper and lower bounds listed in the table.

influencing the proton chemical shift is the protonation of the imidazole ring to which it is attached. The pK_a values reported in Table 2 for His-116 have for assumptions that the imidazole behaves as a thermodynamically independent site and that broadening affects its pK_a negligibly. With the caveat that His-116 has unexplained features, this residue has the highest enthalpy of ionization, 37 kJ mol^{-1}, and the smallest entropy change, -6 J K^{-1} mol^{-1} (Table 3).

DISCUSSION

Thermodynamic parameters of ionization

Several facts have emerged from fundamental studies of the energetics of the dissociation of imidazole in chemically modified histidines and peptides. The dissociation of the imidazole cation into a proton and neutral imidazole is disfavored by a large positive standard enthalpy change and a small negative standard entropy change (Table 3) (Edsall, 1958; Boschcov et al., 1983). This entropy decrease reflects the orientational effect of the imidazole cation on the water dipoles at the cost of disrupting the hydrogen bond network of the solvent. Release of the proton lowers the entropy as the hydrogen bonds are rebuilt. Both entropy and enthalpy are affected by the tautomeric form adopted by the neutral residue (Table 3).

The titration curves of myoglobin show that the standard enthalpy of ionization for the histidines embedded in the protein varies from 16 kJ mol^{-1} to 37 kJ mol^{-1}, in contrast to the standard free energy difference, which ranges from 31 kJ mol^{-1} to 44 kJ mol^{-1}. The narrower $\Delta G°$ range indicates that there is partial compensation of the effects that alter $\Delta H°$. The pK_a values also yield the standard entropy change (Table 3). Enthalpy and entropy are derived

from the same primary measurement, and therefore the two quantities are strongly correlated. Because the $\Delta S°$ values are imprecise, the discussion is limited to His-81 (best determined), His-116, which has the lowest value (close to 0), and His-119, which has the largest negative value. Model compound data, listed in Table 3, serve as reference and aid in the analysis.

The close correspondence between the $\Delta H°$ and $\Delta S°$ measured for His-81 and free histidine is likely to derive from the solvent accessibility of the titrating site and the environment devoid of charges. Unlike His-81, His-119 is partially in a hydrophobic cavity, and the titrating Nδ1 site has limited solvent accessibility. The enthalpy change of His-119 is smaller than that of a normal histidine and tautomeric composition might be reflected in this value. Exclusive formation of the Nϵ2H form in the neutral state implies deprotonation solely at Nδ1. The lower enthalpy of the Nδ1H bond has been established in theory (Mezey et al., 1979) and experiment with the model Nϵ2-Me histidine (Boschcov et al., 1983), and an interpretation for His-119 could be drawn from analogy. However, the entropy of dissociation is more negative than in the model compound and the rationalization of the standard parameters will require further consideration in terms of the hydrophobic environment of His-119.

The complexity of the environmental effects on the thermodynamic parameters also appears for His-116. His-116 has a higher enthalpy of ionization than a free histidine and the lowest entropy change in the set of residues. The tautomeric composition does not account for the high $\Delta H°$ value. The small magnitude of $\Delta S°$ for His-116 hints at minimal net solvent rearrangement or compensating changes in configurational freedom of the side chain with loss of the charge.

The standard enthalpy of ionization measured for His-36 and His-113 illustrates the difficulty of electrostatic modeling. The strength of the coulombic interactions is mediated through the dielectric constant of the solvent and the protein interior (Tanford, 1957; Tanford and Kirkwood, 1957). The dielectric constant of water (D) is ~80 at room temperature and bears a strong inverse relation to T (Archer and Wang, 1990) whereas the apparent dielectric constant inside the protein (D_p) is generally assumed to be small and insensitive to T. Overall, the effect of the lower dielectric constant of the solvent at higher temperatures leaves the Born energy, proportional to $(1/D - 1/D_p)$, relatively unaffected but leads to enhanced charge-charge interactions. Qualitatively, for a free histidine, which experiences no T-dependent charge-charge effect, a rise in T favors deprotonation of the ring (Table 3). The charged state of His-113 is destabilized by electrostatic repulsions from Arg-31, repulsions, which should become stronger as T is raised. Compared with the free histidine, this exaggerates the increase in acidity at higher T. Conversely, the protonated state of His-36 is stabilized by Glu-38 and should become increasingly so as T is raised. This leads to a less pronounced increase in acidity compared with free histidine. The measured en-

TABLE 3   Thermodynamic parameters for histidine ionization

	ΔG°*	ΔH°#	SD§	ΔS°¶	SD§
His	35.1	28.5	0.8	−23	3
NδlMe-His	37.3	31.0	0.8	−22	2
Nε2Me-His	33.8	24.3	0.4	−33	1
His-36	44.1 (43.8, 44.3)	36 (30, 41)	1	−29 (−44, −15)	2
His-48	31.4 (31.0, 31.7)	16 (11, 26)	3	−52 (−66, −40)	10
His-81	39.0 (38.8, 39.3)	31 (26, 37)	1	−28 (−41, −13)	3
His-113	33.0 (32.7, 33.4)	23 (17, 32)	3	−35 (−53, −7)	9
His-116	38.7 (38.4, 39.0)	37 (32, 43)	1	−6 (−18, +7)	4
His-119	36.7 (36.5, 37.0)	20 (15, 26)	1	−58 (−72, −42)	2

*Free energy of ionization (HisH$^+$ = His + H$^+$) in kJ mol^{-1} at 288 K calculated from the data in Table 2. For the model compounds, values are calculated from Boschcov et al. (1983) and with the assumption that ΔC_p° is 0. Lower and upper values were calculated from the standard deviation on the pK$_a$ (Table 2).

#Enthalpy of ionization calculated from the data in Table 2 and linear regression (Eq. 1). Values are in kJ mol^{-1}. For the model compounds, the values are from Boschcov et al. (1983). Isotopic effects may alter these values by approximately 10% (Chervenak and Toone, 1994). No correction was attempted. Upper and lower values were obtained from graphical estimates (Shoemaker et al., 1989).

§Standard deviation of the fit.

¶Entropy of ionization calculated from the data in Table 2 and linear regression (Eq. 2). Values are in J K^{-1} mol^{-1}. For the model compounds, the values are from Boschcov et al. (1983). Upper and lower values were obtained from graphical estimates (Shoemaker et al., 1989).

thalpy changes, low for His-113 and high for His-36, are not consistent with these predictions and cannot be understood solely on the basis of the temperature response of the solvent dielectric.

To analyze further the standard parameters of ionization, it is useful to recognize that the proton dissociation is influenced by several factors and that a correlation between the physics of the reaction and the experimentally measured quantities can be achieved by decomposition into intrinsic and extrinsic components. The intrinsic (or nominal) component arises from energy differences between the reactants and products in the absence of the solvent whereas the extrinsic component is due to solvent-solute interactions (Grunwald and Steel, 1995). This classification is not unique but is adequate for a one-step dissociation reaction. Formally, it can be expressed as

$$\Delta H^{\circ} = \Delta H_{nom} + \Delta H_{sol}. \qquad (4)$$

For an imidazole side chain in the protein, the magnitude of ΔH_{sol} is thought to be mediated largely by solvent accessibility. For simplicity, free energy and entropy components will be partitioned in the same way:

$$\Delta G^{\circ} = \Delta G_{nom} + \Delta G_{sol}, \qquad (5)$$

$$\Delta S^{\circ} = \Delta S_{nom} + \Delta S_{sol}. \qquad (6)$$

Compensation of ΔH_{sol} by ΔS_{sol} removes the influence of solvent from the total free energy change ΔG°. In homologous series, compensation is often demonstrated by the linearity of a ΔH° versus ΔS° plot (Lumry and Rajender, 1970). The slope of the line (β) is close to room temperature when compensated effects dominate the thermodynamics and ΔG° is small compared with ΔH_{sol} (Grunwald and Steel, 1995). Homologous histidine-containing peptides have been reported to yield a β value of 250 K and therefore exhibit compensation (Juliano and Paiva, 1974). Where tight correlation among thermodynamic quantities is an

issue, a plot of pK$_a$(T$_1$) versus pK$_a$(T$_2$), though perhaps too stringent (Lumry and Rajender, 1970), is recommended to extract compensation parameters (Exner, 1975). Compensation then takes the form:

$$pK_a(T_1, i) = \alpha \times f_1(T_1, T_2, \beta) + f_2(T_1, T_2, \beta) \qquad (7)$$
$$\times pK_a(T_2, i).$$

In this equation, α is equivalent to ΔH_{nom} and f_1 and f_2 are two different functions of the temperatures of interest and the compensation parameter β. Fig. 5 shows a rendition of the pK$_a$(T$_1$) versus pK$_a$(T$_2$) plot for published data on angiotensin peptides (Juliano and Paiva, 1974). This set obeys the expectations of compensation as the parameter α is common to the series of compounds. The intercept of the plot provides ΔH_{nom} = 35.5 kJ mol^{-1}, and the points align with a slope controlled by the two temperatures T$_1$ and T$_2$, and β = 250 K. When combined with the ΔH° value of 28.5 kJ mol^{-1} for free histidine, the solvation component is evaluated at approximately −7 kJ mol^{-1} through Eq. 4. The entropy quantity compensating this enthalpy value is −28 J K^{-1} mol^{-1}, which is close to the standard value (Table 3). The nominal component of entropy is the remainder, ~5 J K^{-1} mol^{-1}. These rough estimates will provide a basis for comparing the protein values.

Fig. 5 also contains the data on the histidines of Mb. The protein pK$_a$ values are spread wider than the peptide ones and do not fall on the compensation line defined by the peptides. This result is not surprising as in the folded protein the local environment is likely to affect ΔH_{nom} in specific ways. In other words, Eq. 7 does not apply to the protein set as the α parameter is now a function of the histidine. The consequences of changing the nominal component are marked by the two dashed lines in Fig. 5. These were calculated with ΔH_{nom} = 32.5 kJ mol^{-1} (left line) and ΔH_{nom} = 40.5 kJ mol^{-1} (right line) and a common β = 250 K. The relatively small variation in ΔH_{nom} leads to well
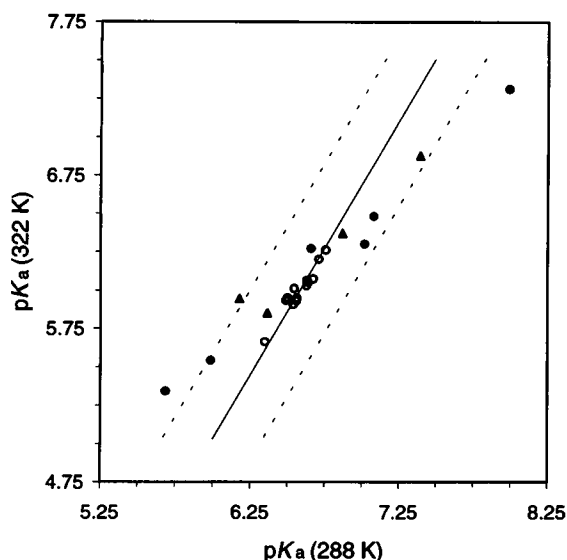
FIGURE 5   Plot of pK_a(288 K) versus pK_a(313 K) for several sets of histidines. O, Histidines in angiotensin derivatives (0.15 M KCl in H_2O) from Juliano and Paiva (1974). The solid line illustrates compensation with a β parameter of 250 K and an α parameter of 35.5 kJ mol^{-1}. The dashed lines are obtained by adding (*right line*) or subtracting (*left line*) 4 kJ mol^{-1} to the α parameter. ●, Histidines in Mb (this work, 0.2 M NaCl in ^2H_2O). ▲, Histidines in human lysozyme (0.1 M NaCl in ^2H_2O; Cohen, 1969) and in ribonuclease A (0.2 M NaCl in ^2H_2O; Westmoreland et al., 1975).

TABLE 4   Solvent contribution to enthalpy and entropy of histidine ionization in myoglobin

Residue*	ΔS_{sol}[#]	ΔH_{sol}[§]	ΔH_{nom}[¶]
His	−28	−7	36
His-36	−34	−9	45
His-48	−57	−14	30
His-81	−33	−8	39
His-113	−40	−10	33
His-116	−11	−3	40
His-119	−63	−16	36

*Tautomeric mixtures as listed in Table 1.
[#]Values in kJ K^{-1} mol^{-1} estimated from Table 3 and equal to $\Delta S° - 5$ kJ K^{-1} mol^{-1}.
[§]Values in kJ mol^{-1} equal to $\beta \Delta S_{sol}$.
[¶]Values in kJ mol^{-1} estimated from Table 3 and equal to $\Delta H° - \Delta H_{sol}$.

resolved lines. The Mb data suggest the histidines in the protein should be compared each with their own compensation line rather than with each other as customary for a homogeneous family of compounds. In this view, His-48 and His-113, to the left of the peptide line would have lower ΔH_{nom} value, whereas His-36 and His-116, to the right of it, would have higher ΔH_{nom} value. The triangles in Fig. 5 represent data points from ribonuclease (Westmoreland et al., 1975) and lysozyme (Cohen, 1969) to show that the trend is not unique to Mb. Overall, the protein data points are below the line defined by $pK_a(T_1) = pK_a(T_2)$ (or $\Delta H° = 0$). This is a result of $\Delta H° > 0$ for all residues. The slope is smaller than 1, indicating that there is a scaling of $\Delta H°$ with $\Delta G°$: the lower the pK_a ($\Delta G°$), the lower $\Delta H°$. This tends to normalize the histidine pK_a to that of a free histidine as T is raised.

Two assumptions will be made to apply the peptide results to the folded protein: 1) ΔS_{nom} is a small invariant quantity approximated by the free histidine value (5 J K^{-1} mol^{-1}) and 2) the solvent contributions compensate, that is, $\Delta H_{sol} = \beta \Delta S_{sol}$. The first assumption is put forth because the nominal value corresponding to a single bond breaking event is thought to be constant and small (Edsall, 1958; Jencks, 1987). The second assumption is supported by the peptide studies mentioned above (Juliano and Paiva, 1974) and by thermodynamic arguments (Grunwald and Steel, 1995). With these assumptions, it becomes possible to estimate ΔH_{sol} and ΔH_{nom} at each site; values are listed in Table 4. The estimated ΔH_{sol} values range from −16 kJ mol^{-1} (His-119) to −4 kJ mol^{-1} (His-116). ΔH_{nom} domi-

nates $\Delta H°$ to different extents. Extremes of behavior are observed in His-116, where solvation effects are negligible, and in His-48 and His-119, where they are enhanced compared with the free histidine.

In the case of His-119, the observed enthalpic partitioning is in qualitative agreement with a reduced solvation of the side chain, which also rationalizes the large negative standard entropy change. Reduced accessibility implies that a greater number of solvent interactions should be formed on going from the cation to the neutral species. The nominal value of the enthalpy is 36 kJ mol^{-1}. Breaking the Nδ1H bond is associated with a small total enthalpy change in the model compound Nϵ2Me-His (Table 3); however, the corresponding nominal component cannot be evaluated for lack of adequate ΔS_{nom} and β. Thus, it is difficult to assess the effect of the low polarity environment of His-119 on the dissociating NH$^+$ bond.

In contrast to His-119, His-116 does not comply readily with a solvent accessibility interpretation. If simple scaling of the enthalpy change held, His-116, which appears partially hindered and has nonnegligible populations of the two tautomeric states in the neutral form, should exhibit a lower ΔH_{sol} than the reference. This is not observed. With its reduced $\Delta S°$ and large $\Delta H°$, His-116 resembles the model compound cyclo-Phe-His (Arena et al., 1992). The explanation in this molecule involves pH-dependent interactions between the two side chains. Site 116 also might experience a conformational rearrangement of the side chain through its titration or the titration of a nearby group.

The complexity of behavior and difficulty of interpretation could stem from several origins. Assumption 1, which states that ΔS_{nom} is small and invariant, might not hold strictly and therefore invalidate the calculated solvent contribution. A variation in ΔS_{nom} could arise from a configurational component to the entropy, distinct in the neutral and the protonated form. It has also been suggested that nearby titratable sites could compromise the scaling of the hydration effect with accessible surface area (Hempel et al., 1995). This invalidates assumption 2 indirectly, by making β a variable rather than a constant. Other reasons could be invoked to question the extent of compensation, in particu-

lar for buried side chains. The magnitude of the $\Delta H°$ changes is not sufficiently larger than that of the $\Delta G°$ changes for an assessment to be made.

The merit of other assumptions is open to question. For example, the change in heat capacity accompanying the ionization process is taken to be zero. Although this is acceptable for an exposed histidine where solvent participation is negligible, structure-dependent extents of solvation in the protonated and neutral states may lead to different values in the native protein. A limitation of the NMR method is the inability to measure small $\Delta Cp°$ values in a narrow T range. However the variations in the experimentally determined $\Delta S°$, and the analysis in terms of ΔS_{sol}, imply a $\Delta Cp°$ value (Shortle et al., 1988). Site-dependent $\Delta Cp°$ parameters would complicate any generalization. It should also be recognized that breaking down the thermodynamic components as in Eqs. 4–6 is valid when there is no correlation between the terms, but it is conceivable that the intrinsic and solvent components are influencing each other (King and King, 1956). The pH-dependent structural changes could confuse further the thermodynamic analysis.

Temperature dependence of proton binding

In the thermal denaturation of metMbH$_2$O the enthalpic contribution from ionization effects is significant over the entire pH range (Privalov, 1979). However, the absence of experimental data in the intermediate pH range (Hermans and Rialdi, 1965; Kelly and Holladay, 1990) has prevented a complete characterization of the role of all of the histidines in the protein. The results in this study can be extended to gain partial insight into the contributions of the histidines in the native and unfolded states in the neutral pH range. This comparison should establish the differential number of bound protons under all conditions of pH and T and help assess the role of protonation in folding equilibria (Barrick and Baldwin, 1993; Yang and Honig, 1993; Barrick et al., 1994; Yang and Honig, 1994) in the pretransition zone.

The pK$_a$ and enthalpy values listed in Tables 2 and 3 show that each titratable histidine in myoglobin has its own response to temperature changes. This is illustrated in Fig. 6 A with a plot of total charge borne by the six titratable myoglobin histidines versus T and pH, constructed from experimentally determined titration curves. To unfold myoglobin in the T and pH ranges of interest, it is necessary to add a chemical denaturant. The validity of extrapolation of pK$_a$ and $\Delta H°$ to pure water is questionable and the pK$_a$ and $\Delta H°$ parameters of histidines in the unfolded state are not readily determined. A practical approach with limitations is to mimic the unfolded state of each histidine with a peptide centered about the residue of interest. Such preliminary peptide data indicate that the pK$_a$ shifts due to the inductive effects is not greater than 0.5 units. Thus, free histidine may serve as a first approximation, and the unfolded state will be represented by six generic histidine groups (Fig. 6 B) to
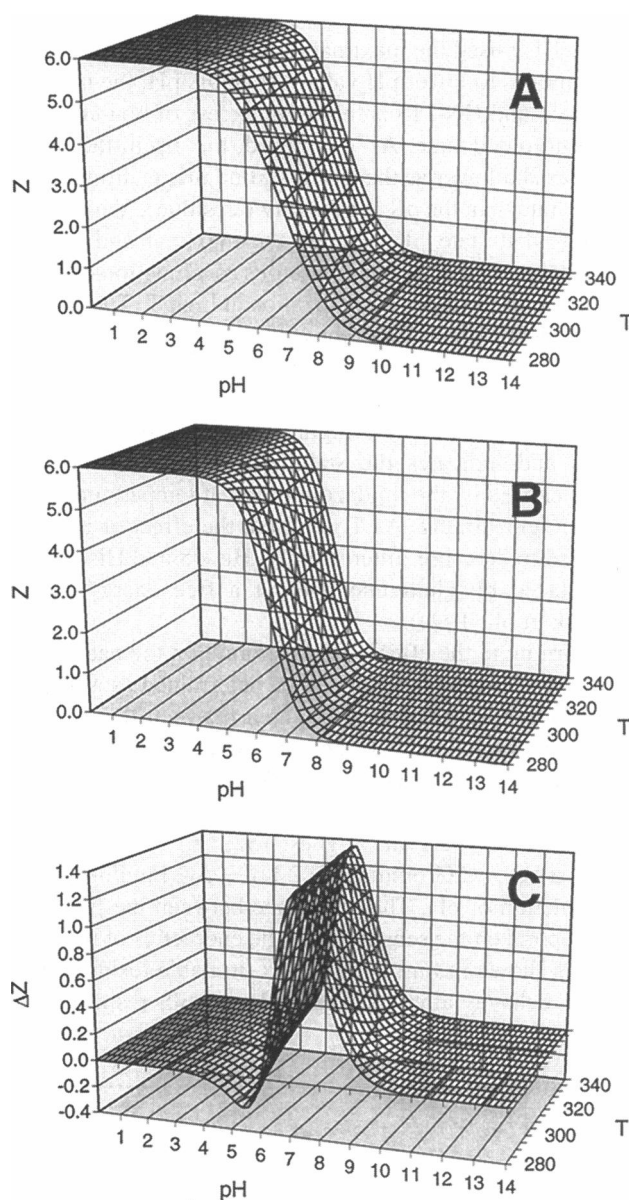

FIGURE 6 Fraction protonated surface calculated as a function of temperature and pH for the following: (A) the six titrating histidines of horse Mb using fitted parameters listed in Tables 2 and 3 and the legend of Fig. 3; (B) free histidine with generic parameters from Boschcov et al. (1983), multiplied by a factor of six; (C) the difference between the surfaces calculated in A and B. A positive ΔZ value means that native Mb carries an excess of protons compared with the unfolded state.

demonstrate the potential of the method. These histidines are taken to behave according to the parameters listed in Table 3, with no correction for solvent isotope composition (Chervenak and Toone, 1994). The shift and slope of the protein surface of Fig. 6 A compared with the scaled peptide surface of Fig. 6 B reveals the influence of the abnormal residues, His-36, His-48, and His-113. Fig. 6 C displays the change in the number of bound protons upon unfolding calculated from the difference between the two surfaces.

At high pH, the contribution of His-36 appears as an excess of bound protons for the folded state. The free

histidine has an enthalpy of ionization smaller than His-36, and as T is raised the maximal discrepancy between the two states moves to lower pH value. At acidic pH, the influence of His-48 and His-113 is felt as an excess of bound protons in the unfolded state. As T is raised, the dip in the surface becomes shallower as the free histidine pK_a is dropping at a steeper rate than the pK_a of these two residues. Variations in the unfolded state pK_a change the maximal and minimal differential number of bound protons as a function of pH but not the trend toward a normalization at high T. The effect of systematic histidine mutations on native state stability of apomyoglobin has been investigated by Baldwin and co-workers (Barrick et al., 1994). The replacement of His-36 by a glutamine leads to a higher sensitivity to H^+ concentration and indicates the stabilizing role of the positive charge carried by the imidazolium ion at temperatures close to room temperature. As T is raised, the effect of His-36 is expected to decrease. Interestingly, His-48 and His-113 can be replaced by glutamine without a free energy penalty (Barrick et al., 1994).

Returning to the effect of temperature on the native state, the work of proton loading can be determined as a function of saturation by evaluating the area between the standard-state ligand axis (pH = 0) and the binding curves of Fig. 3 (Wyman, 1964; Privalov, 1979; Wyman and Gill, 1990). This integration of the experimental data was performed at the lowest (288 K) and highest (322 K) temperatures to derive $\Delta\Delta G = \Delta G(\text{binding, 322 K}) - \Delta G(\text{binding, 288 K})$ as a function of pH. The difference between the two quantities reports on the sensitivity of the energetics of the site to T and is shown in Fig. 7 for the six titratable residues. Each residue behaves after its own fashion with respect to the

maximal difference attained, the pH coordinate of this maximum, and the width of the transition zone. The summed up $\Delta\Delta G$ contributions span a broad pH range and produce a maximal effect of $\sim$40 kJ mol^{-1} near pH = 6.8. For comparison, free histidine displays a $\Delta\Delta G$ of 12 kJ mol^{-1}, centered at $\sim$pH 6.6. The maximal differential work in the folded protein is lower than that provided by the scaled-up free histidine (72 kJ mol^{-1}). With a refined model for the unfolded state instead of the simplistic free histidine, it will be possible to evaluate this effect and, with the appropriate thermodynamic cycle, ultimately make the connection with free energies of unfolding of the protein (Privalov, 1979). In the absence of these data, it can nevertheless be seen that the protonation of the six histidines contributes significantly to changes in free energy in the pre-denaturation zone.

CONCLUSIONS

1) The effective enthalpy of histidine ionization can be measured on a site by site basis in myoglobin by NMR spectroscopy. The advantage of the method is that the native protein can be studied directly in solution. The evidence from NMR experiments suggests that the average conformation over the entire T range resembles the native structure at room temperature. However, structural perturbations and shifts in conformational and tautomeric distribution at higher T may be spectroscopically silent. Therefore one should view the experimentally measured pK_a and $\Delta H°$ values as weighted averages. The built-in complexity due to this factor will prove to be a challenge in modeling the pK_a values and their dependence on T.

2) The enthalpy of histidine ionization can be partitioned into nominal and solvation parts provided that compensation of solvent effects applies. Insight into the contribution of solvation for a charged group in a protein is thus obtained. Within the validity of this approach, it appears that solvation effects are intricate. Theoretical and experimental characterization will be necessary to distinguish among partial compensation, heat capacity effects, and other contributions.

3) With a knowledge of the tautomeric state of each histidine, it becomes possible to interpret the effect of the protein environment on the standard free energy for proton dissociation. For example, His-36 adopts predominantly the tautomeric state with a higher pK_a so that the free energy difference contributed by protein charges (titrating or not) and the Born term amounts to only 7.8 − 6.6 = 1.2 pH units (Tables 2 and 3).

4) Free energy of proton loading can be estimated as a function of T in the pre-denaturation range. To complete the study and compare with the unfolded state properties, model compound data collection is being pursued.

5) The temperature response of the protein-solvent system is not easily described within the framework of existing electrostatic models. There is obvious need for a more comprehensive role of the solvent at the microscopic level as illustrated in this study.
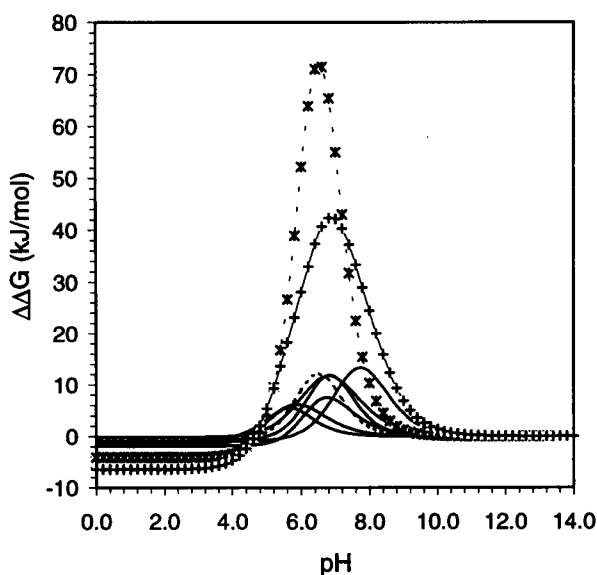

FIGURE 7   Change in free energy of proton loading as a function of pH and temperature. Individual histidines are marked in solid lines without distinction. Free histidine is marked in dashed lines, and the sum of six such histidines is given by - - * - -. The sum of the contributions from the six titrating Mb histidines follows —+—.

The potential of combined pH and temperature studies of proteins has not been fully realized owing to limited availability of experimental data. It is hoped that similar studies on model compounds and proteins from different sources will assist in a complete definition of the mechanistic and structural role of ionizable residues in their native environment.

REFERENCES

Acampora, G., and J. Hermans. 1967. Reversible denaturation of sperm whale myoglobin. I. Dependence on temperature, pH, and composition. *J. Am. Chem. Soc.* 89:1543–1552.

Allewell, N. M., and H. Oberoi. 1991. Electrostatic effects in protein folding, stability, and function. *Methods Enzymol.* 202:3–19.

Archer, D. G., and P. Wang. 1990. The dielectric constant of water and Debye-Hückel limiting law slopes. *J. Phys. Chem. Ref. Data.* 19: 371–411.

Arena, G., G. Impellizzeri, G. Maccarrone, G. Pappalardo, D. Sciotto, and E. Rizzarelli. 1992. Thermodynamics and 1H NMR study of proton complex formation of histidine-containing cyclopeptides in aqueous solution. *J. Chem. Soc. Perkin Trans.* 154:371–376.

Barrick, D., and R. L. Baldwin. 1993. Three-state analysis of sperm whale apomyoglobin folding. *Biochemistry.* 32:3790–3796.

Barrick, D., F. M. Hughson, and R. L. Baldwin. 1994. Molecular mechanisms of acid denaturation: the role of histidine residues in the partial unfolding of apomyoglobin. *J. Mol. Biol.* 237:588–601.

Bashford, D., D. A. Case, C. Dalvit, L. Tennant, and P. E. Wright. 1993. Electrostatic calculations of side-chain pK$_a$ values in myoglobin and comparison with NMR data for histidines. *Biochemistry.* 32:8045–8056.

Bhattacharya, S., S. F. Sukits, K. L. MacLaughlin, and J. T. J. Lecomte. 1997. The tautomeric state of histidines in myoglobin. *Biophys. J.* 73:3230–3240.

Boschcov, P. W., W. S. Seodel, J. Muradian, M. Tominaga, A. C. M. Paiva, and L. Juliano. 1983. Ionization constants and thermodynamic parameters of histidine and derivatives. *Bioorg. Chem.* 12:34–44.

Botelho, L. H., S. H. Friend, J. B. Matthew, L. D. Lehman, G. I. H. Hanania, and F. R. N. Gurd. 1978. Proton nuclear magnetic resonance study of histidine ionizations in myoglobins of various species: comparison of observed and computed pK values. *Biochemistry.* 17:5197–5205.

Breslow, E. 1964. Changes in side chain reactivity accompanying the binding of heme to sperm whale apomyoglobin. *J. Biol. Chem.* 239: 486–496.

Brunori, M., G. Amiconi, E. Antonini, J. Wyman, R. Zito, and R. Fanelli. 1968. The transition between 'acid' and 'alkaline' ferric heme proteins. *Biochim. Biophys. Acta.* 154:315–322.

Carver, J. A., and J. H. Bradbury. 1984. Assignment of 1H NMR resonances of histidine and other aromatic residues in met-, cyano-, oxy-, and (carbon monoxy)myoglobins. *Biochemistry.* 23:4890–4905.

Cavanagh, J., and M. Rance. 1992. Suppression of cross-relaxation effects in TOCSY spectra via a modified DIPSI-2 mixing sequence. *J. Magn. Reson.* 96:670–678.

Chervenak, M. C., and E. J. Toone. 1994. A direct measure of the contribution of solvent reorganization to the enthalpy of ligand binding. *J. Am. Chem. Soc.* 116:10533–10539.

Cho, K. C., H. T. Poon, and C. L. Choy. 1982. The thermodynamics of myoglobin: stability effects of axial ligand. *Biochim. Biophys. Acta.* 701:206–215.

Cocco, M. J., Y.-H. Kao, A. T. Phillips, and J. T. J. Lecomte. 1992. Structural comparison of apomyoglobin and metaquomyoglobin: pH titration of histidines by NMR spectroscopy. *Biochemistry.* 31: 6481–6491.

Cohen, J. S. 1969. Proton magnetic resonance studies of human lysozyme. *Nature.* 223:43–6.

Dalvit, C., and P. E. Wright. 1987. Assignment of resonances in the ¹H nuclear magnetic resonance spectrum of the carbon monoxide complex of sperm whale myoglobin by phase-sensitive two-dimensional techniques. *J. Mol. Biol.* 194:313–327.

Derome, A., and M. Williamson. 1990. Rapid-pulsing artifacts in double-quantum-filtered COSY. *J. Magn. Reson.* 88:177–185.

Dill, K. 1990. Dominant forces in protein folding. *Biochemistry.* 29: 7133–7155.

Edsall, J. T. 1958. Biophysical Chemistry. Academic Press, New York.

Evans, S. V., and G. D. Brayer. 1990. High-resolution study of the three-dimensional structure of horse heart metmyoglobin. *J. Mol. Biol.* 213:885–897.

Exner, O. 1975. Statistics of the enthalpy-entropy relationship. I–V. The enthalpy entropy relationship in organic reactions. *Coll. Czech. Chem. Commun.* 40:2762–2791.

George, P., and H. Hanania. 1952. The ionization of acidic metmyoglobin. *Biochem. J.* 52:517–523.

Grunwald, E., and C. Steel. 1995. Solvent reorganization and thermodynamic enthalpy-entropy compensation. *J. Am. Chem. Soc.* 117: 5687–5692.

Gurd, F. R. N., S. H. Friend, T. M. Rothgeb, R. S. Gurd, and H. Scouloudi. 1980. Electrostatic stabilization in sperm whale and harbor seal myoglobins. *Biophys. J.* 10:65–75.

Hartmann, H., F. Parak, W. Steigemann, G. A. Petsko, and D. R. Ponzi. 1982. Conformational substates in a protein: structure and dynamics of metmyoglobin at 80 K. *Proc. Natl. Acad. Sci. U.S.A.* 79:4967–4971.

Hempel, J. C., R. M. Fine, M. Hassan, W. Ghoul, A. Guaragna, S. C. Koerber, Z. Li, and A. T. Hagler. 1995. Conformational analysis of endothelin-1: effects of solvation free energy. *Biopolymers.* 36:283–301.

Hermans, J., Jr., and G. Rialdi. 1965. Heat of ionization and denaturation of sperm-whale myoglobin determined with a microcalorimeter. *Biochemistry.* 4:1277–1281.

Hunkapiller, M. W., S. H. Smallcombe, D. R. Whitaker, and J. H. Richards. 1973. Carbon nuclear magnetic resonance studies of the histidine residue in α-lytic protease: implications for the catalytic mechanism of serine proteases. *Biochemistry.* 12:4732–4743.

Jencks, W. P. 1987. Catalysis in Chemistry and Enzymology. Dover Publications, New York.

Juliano, L., and A. C. M. Paiva. 1974. Conformation of angiotensin II in aqueous solution: titration of several peptide analogs and homologs. *Biochemistry.* 13:2445–2450.

Kalinowski, H. O., S. Berger, and S. Braun. 1991. Carbon-13 NMR Spectroscopy. Wiley, New York.

Kao, Y.-H. 1994. A study of metaquomyoglobin in solution by NMR spectroscopy. Structural properties and histidine ionization. Ph.D. thesis. The Pennsylvania State University, University Park, PA. 242 pp.

Kelly, L., and L. A. Holladay. 1990. A comparative study of the unfolding thermodynamics of vertebrate metmyoglobins. *Biochemistry.* 29: 5062–5069.

Kesvatera, T., B. Jonsson, E. Thulin, and S. Linse. 1996. Measurement and modelling of sequence-specific pK$_a$ values of lysine residues in calbindin D$_{9k}$. *J. Mol. Biol.* 259:828–839.

Khare, D., P. Alexander, J. Antosiewicz, P. Bryan, M. Gilson, and J. Orban. 1997. pK$_a$ measurements from nuclear magnetic resonance for the B1 and B2 immunogobulin G-binding domains of protein G: comparison with calculated values for nuclear magnetic resonance and x-ray structures. *Biochemistry.* 36:3580–3589.

King, E. J., and G. W. King. 1956. The thermodynamics of ionization of amino acids. II. The ionization constants of some N-acyl amino acids. *J. Am. Chem. Soc.* 78:1089–1099.

Kuczera, K., J. Kuryian, and M. Karplus. 1990. Temperature dependence of the structure and dynamics of myoglobin: a simulation approach. *J. Mol. Biol.* 192:133–154.

Kuriyan, J., S. Wilz, M. Karplus, and G. A. Petsko. 1986. X-ray structure and refinement of carbonmonoxy (Fe-II) myoglobin at 1.5 Å resolution. *J. Mol. Biol.* 192:133–154.

Lecomte, J. T. J., Y.-H. Kao, and M. J. Cocco. 1996. The native state of apomyoglobin described by proton NMR spectroscopy: the A-B-G-H interface of wild-type sperm whale apomyoglobin. *Proteins Struct. Funct. Genet.* 25:267–285.

Lee, B., and F. M. Richards. 1971. The interpretation of protein structures: estimation of static accessibility. *J. Mol. Biol.* 55:379–400.

Live, D. H., D. G. Davis, W. C. Agosta, and D. Cowburn. 1984. Long range hydrogen bond mediated effects in peptides: ^{15}N NMR study of gramicidin S in water and organic solvents. *J. Am. Chem. Soc.* 106: 1939–1941.

Lumry, R., and S. Rajender. 1970. Enthalpy-entropy compensation phenomena in water solutions of proteins and small molecules: a ubiquitous property of water. *Biopolymers.* 9:1125–1227.

Makhatadze, G. I., and P. L. Privalov. 1993. Contribution of hydration to protein folding thermodynamics. I. The enthalpy of hydration. *J. Mol. Biol.* 232:639–659.

Makhatadze, G. I., and P. L. Privalov. 1994. Hydration effects in protein unfolding. *Biophys. Chem.* 51:291–304.

Markley, J. 1975. Observation of histidine residues in proteins by means of nuclear magnetic resonance spectroscopy. *Acc. Chem. Res.* 8:70–80.

Martin, M. L., G. J. Martin, and J.-J. Delpuech. 1980. Practical NMR Spectroscopy. Heyden, Philadelphia.

Meeker, A. K., B. García-Moreno, and D. Shortle. 1996. Contributions of the ionizable amino acids to the stability of staphylococcal nuclease. *Biochemistry.* 35:6443–6449.

Mezey, P. G., J. J. Ladik, and S. Suhai. 1979. Non-empirical SCF-MO studies on the protonation of biopolymer constituents. I. Protonation of amino acids. *Theor. Chim. Acta.* 51:323–329.

Müller, L. 1979. Sensitivity enhanced detection of weak nuclei using heteronuclear multiple quantum coherence. *J. Am. Chem. Soc.* 101: 4481–4484.

Oda, Y., T. Yamazaki, K. Nagayama, S. Kanaya, Y. Kuroda, and H. Nakamura. 1994. Individual ionization constants of all the carboxyl groups in ribonuclease HI from *Escherichia coli* determined by NMR. *Biochemistry.* 33:5275–5284.

Piotto, M., V. Saudek, and V. Sklenar. 1992. Gradient-tailored excitation for single-quantum NMR spectroscopy of aqueous solutions. *J. Biomol. NMR.* 2:661–665.

Pople, J. A., W. G. Schneider, and H. J. Bernstein. 1959. High-Resolution Nuclear Magnetic Resonance. McGraw-Hill, New York.

Privalov, P. 1979. Stability of proteins: small globular proteins. *Adv. Prot. Chem.* 33:167–241.

Privalov, P. L., Y. V. Griko, S. Y. Venyaminov, and V. P. Kutyshenko. 1986. Cold denaturation of myoglobin. *J. Mol. Biol.* 190:487–498.

Privalov, P. L., and G. I. Makhatadze. 1993. Contribution of hydration to protein folding thermodynamics. II. The entropy and Gibbs energy of hydration. *J. Mol. Biol.* 232:660–679.

Quirt, A. R., J. R. J. Lyerla, I. R. Peat, J. S. Cohen, W. F. Reynolds, and M. H. Freedman. 1974. Carbon-13 nuclear magnetic resonance titration shifts in amino acids. *J. Am. Chem. Soc.* 96:570–574.

Rance, M., and P. E. Wright. 1986. Analysis of ^{1}H NMR spectra of proteins using multiple-quantum coherence. *J. Magn. Reson.* 66: 372–378.

Reynolds, W. F., I. R. Peat, M. H. Freedman, and J. R. Lyerla. 1973. Determination of the tautomeric form of the imidazole ring of L-

histidine in basic solution by carbon-13 magnetic resonance spectroscopy. *J. Am. Chem. Soc.* 95:328–331.

Roberts, G. C. K., D. H. Meadows, and O. Jardetzky. 1969. Nuclear magnetic resonance studies of the structure and binding sites of enzymes. VII. Solvent and temperature effects of the ionization of histidine residues of ribonuclease. *Biochemistry.* 8:2053–2056.

Schaller, W., and A. D. Robertson. 1995. pH, ionic strength, and temperature dependences of ionization equilibria for the carboxyl groups in turkey ovomucoid third domain. *Biochemistry.* 34:4714–23.

Shire, S. J., G. I. H. Hanania, and F. R. N. Gurd. 1974. Electrostatic effects in myoglobin: hydrogen ion equilibria in sperm whale ferrimyoglobin. *Biochemistry.* 13:2967–2979.

Shoemaker, D. P., C. W. Garland, and J. W. Nibler. 1989. Experiments in Physical Chemistry. McGraw-Hill, New York.

Shortle, D., A. K. Meeker, and E. Freire. 1988. Stability mutants of staphylococcal nuclease: large compensating enthalpy-entropy changes for the reversible denaturation reaction. *Biochemistry.* 27:4761–4768.

Shrager, R. I., J. S. Cohen, S. R. Heller, D. H. Sachs, and A. N. Schechter. 1972. Mathematical model for interacting groups in nuclear magnetic resonance titration curves. *Biochemistry.* 11:541–547.

Stigter, D., and K. A. Dill. 1990. Charge effects on folded and unfolded proteins. *Biochemistry.* 29:1262–1271.

Sudmeier, J. L., J. L. Evelhoch, and N. B.-H. Jonsson. 1980. Dependence of NMR lineshape analysis upon chemical rates and mechanisms: implications for enzyme histidine titrations. *J. Magn. Reson.* 40:377–390.

Takano, T. 1977. Structure of myoglobin refined at 2.0 Å resolution. I. Crystallographic refinement of sperm whale metmyoglobin. *J. Mol. Biol.* 110:537–568.

Takano, T. 1984. Refinement of myoglobin and cytochrome *c.* *In* Methods and Applications in Crystallographic Computing. Oxford University Press, Oxford, U.K. 262–272.

Tanford, C. 1957. Theory of protein titration curves. II. Calculation for simple models at low ionic strength. *J. Am. Chem. Soc.* 79:5340–5347.

Tanford, C., and J. G. Kirkwood. 1957. Theory of protein titration curves. I. General equations for impenetrable spheres. *J. Am. Chem. Soc.* 79: 5333–5339.

Westmoreland, D. G., C. R. Matthews, M. B. Hayes, and J. S. Cohen. 1975. Nuclear magnetic resonance titration curves of histidine ring protons: the effect of temperature on ribonuclease. *J. Biol. Chem.* 250:7456–7460.

Wilbur, D. J., and A. Allerhand. 1977. Titration behavior and tautomeric states of individual histidine residues of myoglobin. *J. Biol. Chem.* 252:4968–4975.

Wishart, D. S., C. G. Bigam, J. Yao, F. Abildgaard, H. J. Dyson, E. Oldfield, J. L. Markley, and B. D. Sykes. 1995. ^{1}H, ^{13}C and ^{15}N chemical shift referencing in biomolecular NMR. *J. Biomol. NMR.* 6:135–140.

Wyman, J. 1964. Linked functions and reciprocal effects in hemoglobin: a second look. *Adv. Prot. Chem.* 19:223–286.

Wyman, J., and S. J. Gill. 1990. Binding and Linkage: Functional Chemistry of Biological Macromolecules. University Science Books, Mill Valley, CA.

Yang, A.-S., and B. Honig. 1993. On the pH dependence of protein stability. *J. Mol. Biol.* 231:459–474.

Yang, A.-S., and B. Honig. 1994. Structural origins of pH and ionic strength effects on protein stability: acid denaturation of sperm whale apomyoglobin. *J. Mol. Biol.* 237:602–614.

Yang, F., and G. N. J. Phillips. 1996. Crystal structures of CO-, deoxy- and met-myoglobins at various pH values. *J. Mol. Biol.* 256:762–774.